Journal of Alloys and Compounds 687 (2016) 263–273

Contents lists available at ScienceDirect

Journal of Alloys and Compounds

journal homepage: http://www.elsevier.com/locate/jalcom

A comparative study on the phenomenological and artificial neural network models to predict hot deformation behavior of AlCuMgPb alloy

H.R. Rezaei Ashtiani*, P. Shahsavari

School of Mechanical Engineering, Arak University of Technology, Arak 38135-1177, Iran

ARTICLE INFO

Article history:
Received 30 January 2016
Received in revised form
13 April 2016
Accepted 29 April 2016
Available online 3 May 2016

Keywords:
AlCuMgPb alloy
Hot deformation behavior
Phenomenological models
Artificial neural network

ABSTRACT

The high-temperature deformation behavior of AlCuMgPb alloy was investigated by the hot compression tests over a wide range of deformation temperature (623–773 K) and strain rate (0.005–0.5 s^{-1}). Based on the experimental results, the phenomenological models consist of the Johnson-Cook, Arrhenius-type and Strain-compensation Arrhenius-type constitutive equations and an artificial neural network (ANN) model with a feed forward back propagation learning algorithm were developed for the prediction of the hot deformation behavior of the AlCuMgPb alloy. And then a comparative predictability of the phenomenological models and the trained ANN model were further evaluated in terms of the correlation coefficient(R), average absolute relative error (AARE), root mean square error (RMSE) and relative error. The results showed that the Arrhenius-type constitutive equation could predict the flow stress accurately except under the strain rate of 0.005 s^{-1}. The Strain-compensated Arrhenius-type constitutive equation could represent the elevated temperature flow behavior more accurately than the other investigated phenomenological models consist of Johnson-Cook and Arrhenius-type constitutive equations in the entire processing domain. The results indicated that the trained ANN model is more efficient and accurate in predicting the hot deformation behavior in AlCuMgPb alloy than the investigated phenomenological constitutive equations and offers no physical insight.

© 2016 Published by Elsevier B.V.

1. Introduction

Aluminum alloys and especially the 2000 series alloys are used in various important industries such as automobile and aeronautical applications due to the high strength to weight ratio associated with good fracture toughness, good corrosion resistance and excellent high temperature characteristics. Generally, these series of aluminum alloys will be subject to various hot forming processes, such as rolling, forging, extrusion, and heat treatments [1–3].

The hot deformation processes of materials are a very important step in the manufacture of mechanical components, which affect the final quality of products such as microstructural and mechanical properties and dimensional accuracy [4]. The deformation behavior of materials is related to the metallurgical phenomena such as work hardening and dynamic softening (dynamic recovery and recrystallization) that can occur during hot working processes [5,6]. This complexity of deformation behavior, however, leads to the expectation that deformation can only be accurately calculated with the aid of computer code to model the material's response under the specified loading conditions. For this purpose, constitutive equation is often used to represent flow behaviors of materials in a form that can be used in computer code to model and simulate the mechanical behavior of materials and deformation processes under the prevailing loading conditions [7–13]. In order to obtain the reliable simulation results, it is necessary an accurate model that can correctly describe the relationship between flow stress and processing parameters.

Many researchers have tried to predict the mechanical behavior of materials in the hot working condition using constitutive models. Therefore, various constitutive equations have been proposed to describe the flow behavior, which including phenomenological, physically-based and artificial neural network (ANN) models [14–16]. Recently, Johnson-Cook model has been successfully incorporated in finite element analysis to describe the

* Corresponding author.
E-mail addresses: hr_rezaei@arakut.ac.ir, hrr.ashtiani@gmail.com (H.R.R. Ashtiani).

http://dx.doi.org/10.1016/j.jallcom.2016.04.300
0925-8388/© 2016 Published by Elsevier B.V.

elevated temperature flow behavior of materials due to its simple multiplication form. the Johnson–Cook constitutive model is the most widely known phenomenological model which is used to predict the hot deformation of alloys as a deformation temperature, strain and strain rate dependent model [17] and is successfully used for a variety of materials with different ranges of forming temperature and strain rate.

The hyperbolic sine Arrhenius-type constitutive model, as another phenomenological constitutive model, has been successfully applied to predict the hot deformation behavior of materials [18–20]. The original model has been revised several times to appropriately represent the elevated temperature flow behavior of various alloys. In order to increase the accuracy of prediction of the Arrhenius-type constitutive equations, the effects of strain [21–23] and strain rate [24,25] have been considered in the Arrhenius-type constitutive equations by many researchers. For example, Sloof et al. [21] introduced a strain-dependent parameter into the hyperbolic sine constitutive equation in order to make their model predict the elevated temperature flow behavior of a wrought magnesium alloy more accurately. Lin et al. [24] modified the model to describe the hot deformation behavior of 42CrMo steel over a wide range of strain rates and deformation temperatures by compensation of strain and strain-rate. The artificial neural network (ANN) method provides a novel approach to predict deformation behavior of materials under different conditions. ANN is an artificial intelligence technology to simulate biological processes of human brain. It does not need to postulate a mathematical model or identify its parameters. However, the response of the materials deformation behavior is highly nonlinear at elevated temperatures, and many factors affecting the flow behavior of materials are also nonlinear, which make the accuracy of the flow stress predicted by the regression methods low and the proper range limited. While the attraction of ANN is that they are best suited to solve the problems that are the most difficult to solve by traditional computational methods. ANN is especially suitable for treating complex and non-linear relationships; therefore, ANN has been successfully applied to predict deformation behavior of materials in hot working condition. Neural networks can provide a fundamentally different approach to materials modeling and material processing control techniques than statistical or numerical methods. Recently, some efforts have been made to the applications of a new approach of ANN in the prediction of hot deformation behavior of materials, especially for complex and nonlinear systems [14,26–32]. Chai et al. [26] developed a back propagation ANN model to predict the flow stress of XC45 steel at elevated temperature. Xiao et al. [32] developed a back propagation learning algorithm ANN model to predict the hot deformation behavior of 12Cr3WV steel and showed that the ANN model can predict the flow stress of 12Cr3WV efficiently and accurately.

In this study, the effects of deformation temperatures, strain rates and strain on the hot deformation characteristics of AlCuMgPb alloy are investigated by isothermal hot compression tests in a temperature range from 623 K to 773 K and a strain rate range from 0.005 s^{-1} to 0.5 s^{-1}. The main purpose of this paper is to establish relationships among flow stress, strain, strain rate and deformation temperature through a feed forward back propagation artificial neural network model and three kinds of the phenomenological models consisting of Johnson-Cook (JC), Arrhenius-type and Strain compensation Arrhenius-type models, to predict the hot deformation behavior of AlCuMgPb alloy. Meanwhile a comparative investigation is conducted about predictability of these models and their predictabilities are evaluated based on the relative errors, correlation coefficient (R), root mean square error (RMSE) and average absolute relative error (AARE).

2. Experimental procedure

The chemical composition of the AlCuMgPb alloy employed in this investigation is given in Table 1. Cylindrical specimens were machined with 8 mm in diameter and 12 mm in height in accordance with ASTM E209 [33]. Annealing heat treatment was employed at 713 K for 2 h then cooled at cooling rate of 0.02 K/s to 533 K in a furnace and after that cooled at room temperature in the ambience to achieve proper and similar initial microstructure in aluminum alloy samples which had been hot extruded. The optical micrograph of annealed AlCuMgPb alloy specimen with approximate grain size of 100 μm has been shown in Fig. 1. Thin mica sheets were used as a lubricant material at the contact surface of anvils and specimen to minimize the frictions during hot deformation. The samples were heated to test temperature and were held for 5 min to eliminate thermal gradients at the test temperatures. The uniaxial one-hit hot compression tests were performed at 623–773 K with an interval of 50 K and at strain rates of 0.005 s^{-1}, 0.05 s^{-1} and 0.5 s^{-1} using a Gotech-AI7000 servo-controlled electronic universal testing machine equipped with an electrical resistance furnace. After deformation to strain of 0.6, the specimens were immediately quenched in water to retain the microstructures at elevated temperature.

3. Results and discussion

3.1. Flow stress behavior

The true stress-true strain curves of AlCuMgPb alloy obtained during hot compression test in the temperature range of at 623–773 K and strain rates of 0.005 s^{-1}, 0.05 s^{-1} and 0.5 s^{-1} have been presented in Fig. 2. Obviously, the effects of deformation temperature and strain rate on the flow stress are significant. The increase of strain rate and the decrease of temperature can increase flow stress. Moreover, the effects of strain on the flow stress are clear. During the early stage of the deformation, the flow stress increased rapidly due to work hardening. After reaching the peak flow stress, the curves exhibited remarkable steady stage as a result of equilibrium of work hardening and dynamic softening.

3.2. Phenomenological models

The phenomenological models are defined based on the empirical observations of experimental result and consists of some mathematical functions [14]. In this study, three models of phenomenological models including Johnson-Cook, Arrhenius-type and Strain-compensated Arrhenius-type models are developed base on experimental data from isothermal hot compression tests at a wide range of temperature and strain rate.

3.2.1. Johnson-Cook model

The Johnson-Cook (JC) constitutive model is a phenomenological model, and is successfully used for a variety of materials with different ranges of temperature and strain-rate. The original Johnson–Cook model can be represented as Eq. (1) [14,17].

Table 1
Chemical composition (wt. %) of AlCuMgPb alloy.

Cu	Mg	Pb	Si	Fe	Mn	Cr	Zn	Ti
3.85	0.92	1.12	0.37	0.58	0.25	0.01	0.37	0.01

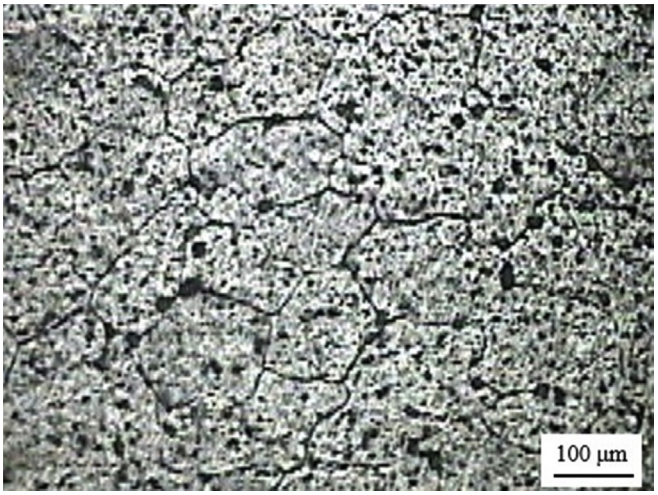

Fig. 1. Optical microstructure of AlCuMgPb alloy after annealing heat treatment.

$$\sigma = (\sigma_0 + B\varepsilon^n)(1 + C\ln\dot{\varepsilon}^*)(1 - T^{*m}) \quad (1)$$

where σ is the equivalent flow stress, ε is the plastic strain, σ_0 is the proof stress at reference strain rate and reference temperature, B is the coefficient of strain hardening, n is the strain hardening exponent, C and m are the material constants which represent the coefficient of strain rate hardening and thermal softening exponent, respectively. $\dot{\varepsilon}^*$ is the dimensionless strain rate, and can be expressed as $\dot{\varepsilon}^* = \dot{\varepsilon}/\dot{\varepsilon}_0$, where $\dot{\varepsilon}$ and $\dot{\varepsilon}_0$ are strain rate and reference strain rate, respectively. T^* is the homologous temperature and expressed as $T^* = (T - T_r)/(T_m - T_r)$, where T, T_m and T_r are the deformation temperature, melting temperature (T_m = 893 K for AlCuMgPb alloy) and reference temperature ($T \geq T_r$), respectively.

In general, the JC constitutive equation considers a set of equations to modeling the mechanical behaviors of materials as the multiplication effects of temperature, strain-rate and strain. This form has a clear physical interpretation consisting of strain hardening, strain-rate hardening and thermal softening as three independent phenomena. So this model does not represent any deformation history consisting of thermal and strain rate history.

In this study, 623 K and 0.5 s^{-1} are taken as the reference temperature and strain rate, respectively to obtain the material constant of the Johnson-Cook model and the value of σ_0 is 75.33 MPa at reference temperature and strain rate.

In order to determine the material constants in Eq. (1), the values of B and n are obtained at reference temperature and strain rate (strain hardening part of the JC model), as:

$$\sigma = \sigma_0 + B\varepsilon^n \quad (2)$$

Taking the natural logarithm on both sides of Eq. (2) gives,

$$\ln(\sigma_0 - \sigma) = \ln(-B) + n\ln\varepsilon \quad (3)$$

By substituting the values of flow stresses and corresponding strain values into Eq. (3) gives relationship between $ln(\sigma_0 - \sigma)$ and $\ln\varepsilon$. So, the values of n and B can be obtained from the slope and intercept of the fitting line shown in Fig. 3, as n = 2.072 and B = −14.379.

After obtaining the values of n and B, Eq. (3) comes as the following at reference temperature

$$\frac{\sigma}{\sigma_0 + B\varepsilon^n} = 1 + C\ln\dot{\varepsilon}^* \quad (4)$$

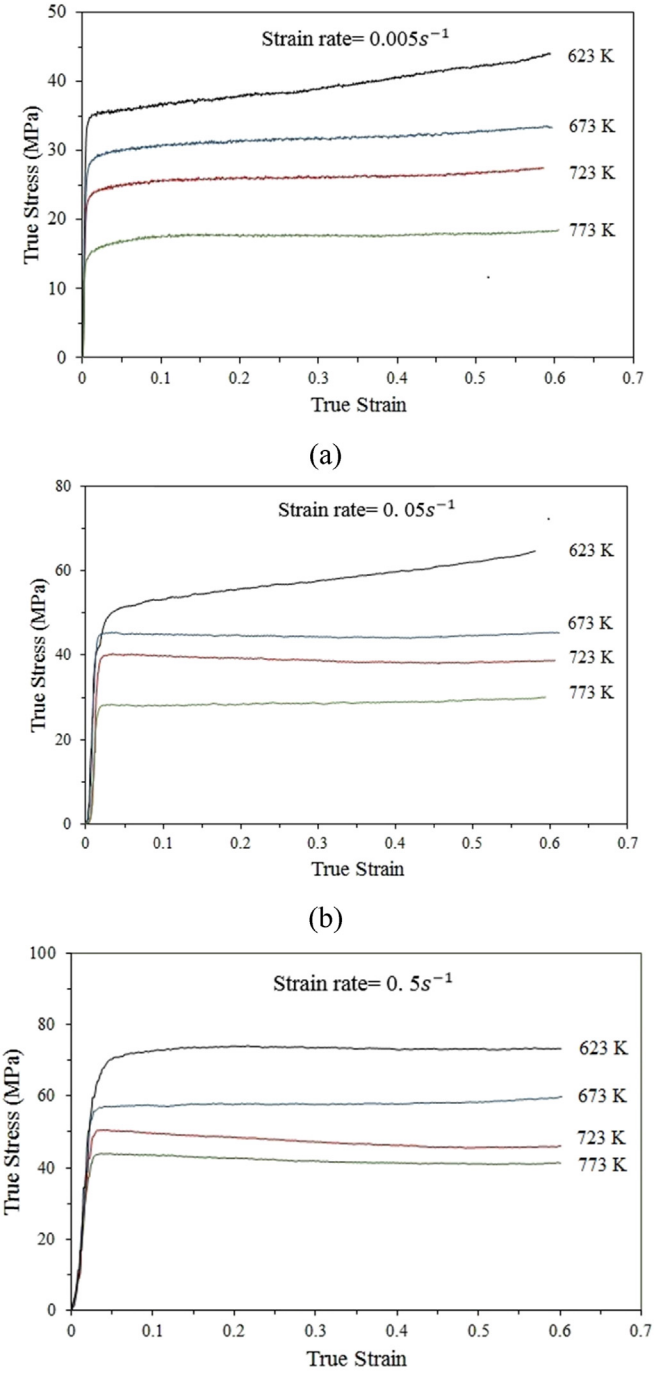

Fig. 2. The true strain-stress curves of AlCuMgPb alloy at various temperature and strain rate of (a) 0.005 s^{-1}, (b) 0.05 s^{-1} and (c) 0.5 s^{-1}.

The relationship between $\sigma/(\sigma_0 + B\varepsilon^n)$ and $\ln\dot{\varepsilon}^*$ can be obtained for a series of strains (0.1–0.6) and strain rates at reference temperature as shown in Fig. 4. The average value of material constant C can be evaluated as 0.096 by linear fitting method.

When the strain rate is 0.5 s^{-1}, Eq. (1) can be rewritten as:

$$\frac{\sigma}{\sigma_0 + B\varepsilon^n} = 1 - T^{*m} \quad (5)$$

Taking the natural logarithm of both sides of Eq. (5) gives:

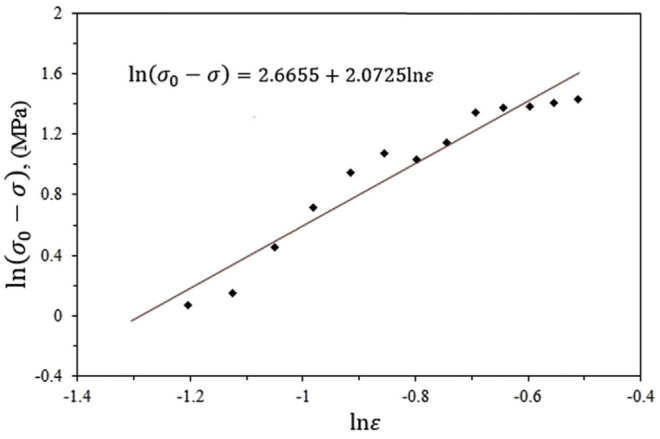

Fig. 3. Relationship between $ln(\sigma_0-\sigma)$ and $\ln\varepsilon$ at 623 K and 0.5 s^{-1}.

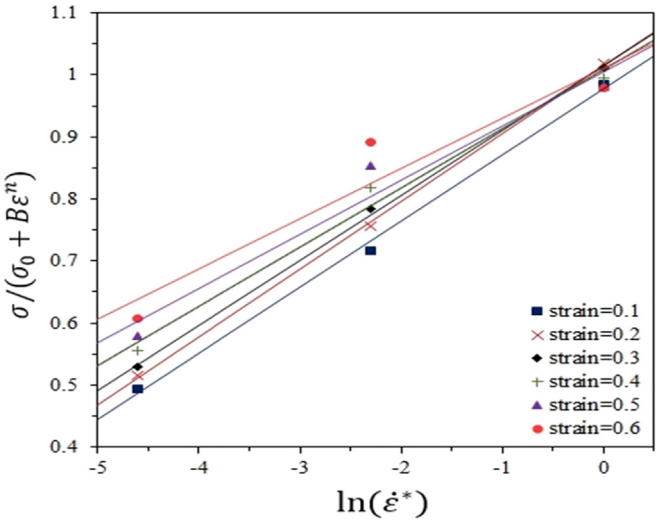

Fig. 4. Relationship between $\sigma/(\sigma_0+B\varepsilon^n)$ and $\ln(\dot{\varepsilon}/\dot{\varepsilon}_0)$.

$$\ln\left[1-\frac{\sigma}{\sigma_0+B\varepsilon^n}\right]=m\ln T^* \tag{6}$$

Finally, the relationship between $\ln[1-\sigma/(\sigma_0+B\varepsilon^n)]$ and $\ln T^*$ can be obtained by substituting the values of stress and strain at different temperature into Eq. (6), as shown in Fig. 5. The average value of material constant m can be obtained 1.349 by liner fitting method.

After determining the material constants of constitutive equation, the Johnson-Cook model can be summarized as follow,

$$\sigma=\left(75.33-14.379\varepsilon^{2.072}\right)\left(1+0.096\ln\dot{\varepsilon}^*\right)\left(1-T^{*1.349}\right) \tag{7}$$

The comparisons between the measured and predicted flow stress of the investigated AlCuMgPb alloy by the Johnson-Cook model under different temperature, strain and strain rate condition have been shown in Fig. 6. As it is observed a fairly good agreement has been obtained between the flow stress values predicted by the Johnson-Cook model and the experimental results.

3.2.2. Arrhenius-type model

The Arrhenius-type model is most widely used to predict flow behavior of materials at high temperatures. The correlation

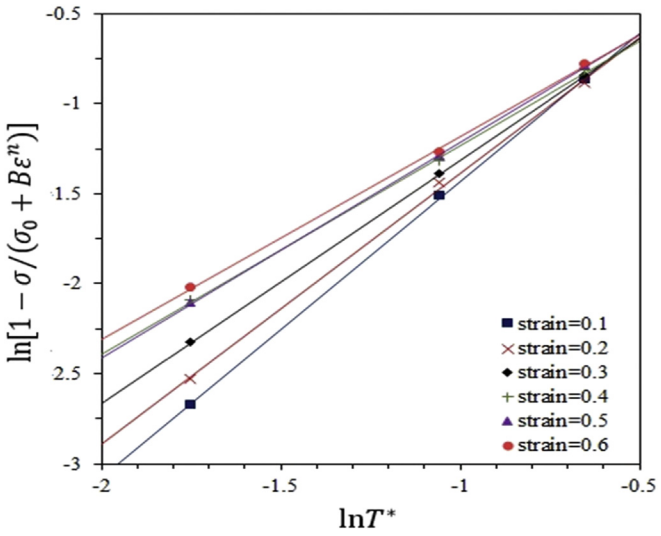

Fig. 5. Relationship between $\ln[1-\sigma/(\sigma_0+B\varepsilon^n)]$ and $\ln T^*$.

between the flow stress (σ), temperature (T) and strain rate ($\dot{\varepsilon}$), could be expressed by the power law (Eq. (8)), the exponential law (Eq. (9)) and the hyperbolic sine-type equation (Eq. (10)) in low stress, high stress and all range of stress levels, respectively, which are given by Eqs. (8)–(10):

$$\dot{\varepsilon}=A_1\sigma^{n'}exp\left(-\frac{Q}{RT}\right)\quad(for\ \alpha\sigma<0.8) \tag{8}$$

$$\dot{\varepsilon}=A_2exp(\beta\sigma)\ exp\left(-\frac{Q}{RT}\right)\quad(for\ \alpha\sigma>1.2) \tag{9}$$

$$\dot{\varepsilon}=A_3[sinh(\alpha\sigma)]^n\ \exp\left(-\frac{Q}{RT}\right)\quad(for\ all\ stress) \tag{10}$$

where $\dot{\varepsilon}$ is the strain rate (s^{-1}), Q is the deformation activation energy ($KJmol^{-1}$), R is the universal gas constant (8.31 J mol^{-1} K^{-1}), T is the absolute temperature (K) and A_1, A_2, A_3, n', n, β and α ($\alpha=\beta/n'$) are the material constants.

The influence of temperature and strain rate on the material deformation behavior can be expressed by Zener–Hollomon parameter (Z) in Eq. (11):

$$Z=\dot{\varepsilon}\exp\left(\frac{Q}{RT}\right) \tag{11}$$

For all the stress level, Eq. (10) can be represented by Eq. (12).

$$Z=\dot{\varepsilon}exp\left(\frac{Q}{RT}\right)=A[\sinh(\alpha\sigma)]^n \tag{12}$$

Then, the flow stress can be rewritten as a function of Zener-Hollomon parameter by using definition of hyperbolic sine law given as Eq. (13) at a particular strain.

$$\sigma=\frac{1}{\alpha}\left\{\left(\frac{Z}{A}\right)^{1/n}+\left[\left(\frac{Z}{A}\right)^{2/n}+1\right]^{1/2}\right\} \tag{13}$$

Finally, the Arrhenius-type model can be summarized as Eq. (14) at strain of 0.1.

$$\begin{cases} \sigma = \dfrac{1}{0.026}\ln\left\{\left(\dfrac{Z}{1.198\times10^{6}}\right)^{1/4.556} + \left[\left(\dfrac{Z}{1.198\times10^{6}}\right)^{2/4.556} + 1\right]^{1/2}\right\} \\ Z = \dot{\varepsilon}\exp\left(\dfrac{104.223\times10^{3}}{RT}\right) \end{cases} \tag{14}$$

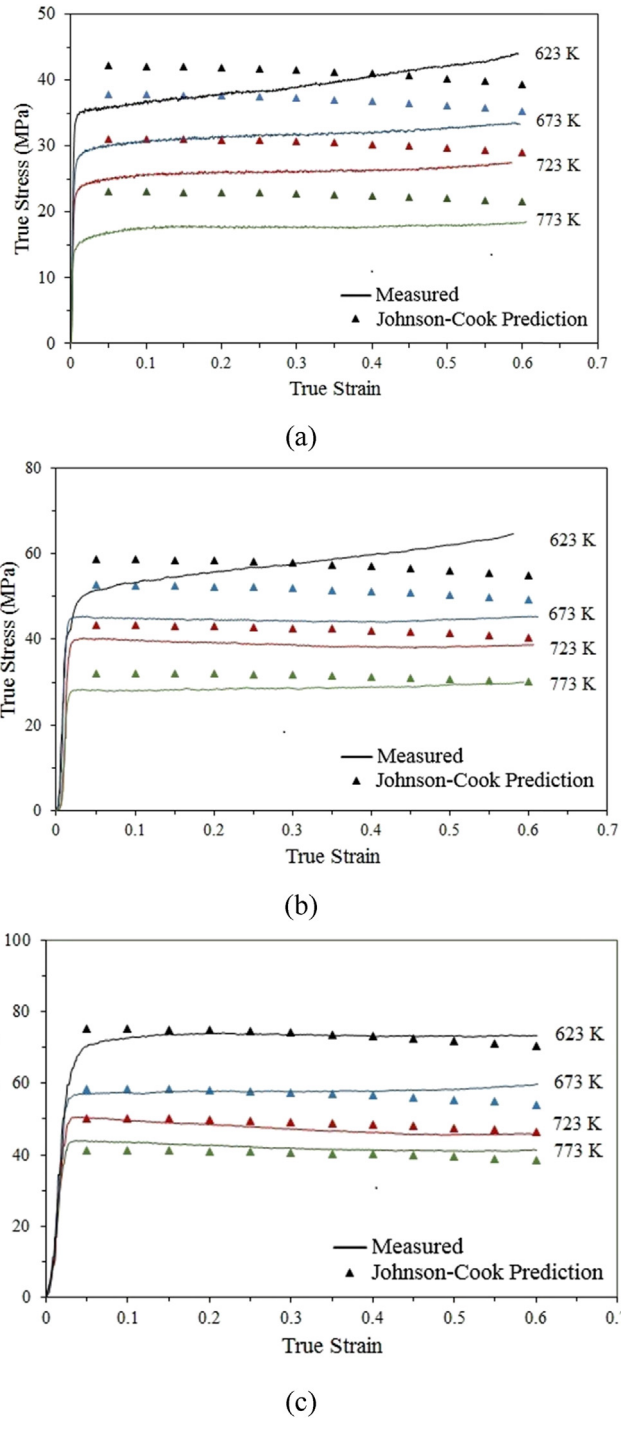

Fig. 6. Comparisons between the measured and predicted flow stress of AlCuMgPb alloy by Johnson-Cook model at different temperatures and strain rate of (a) 0.005 s^{-1}, (b) 0.05 s^{-1} and (c) 0.5 s^{-1}.

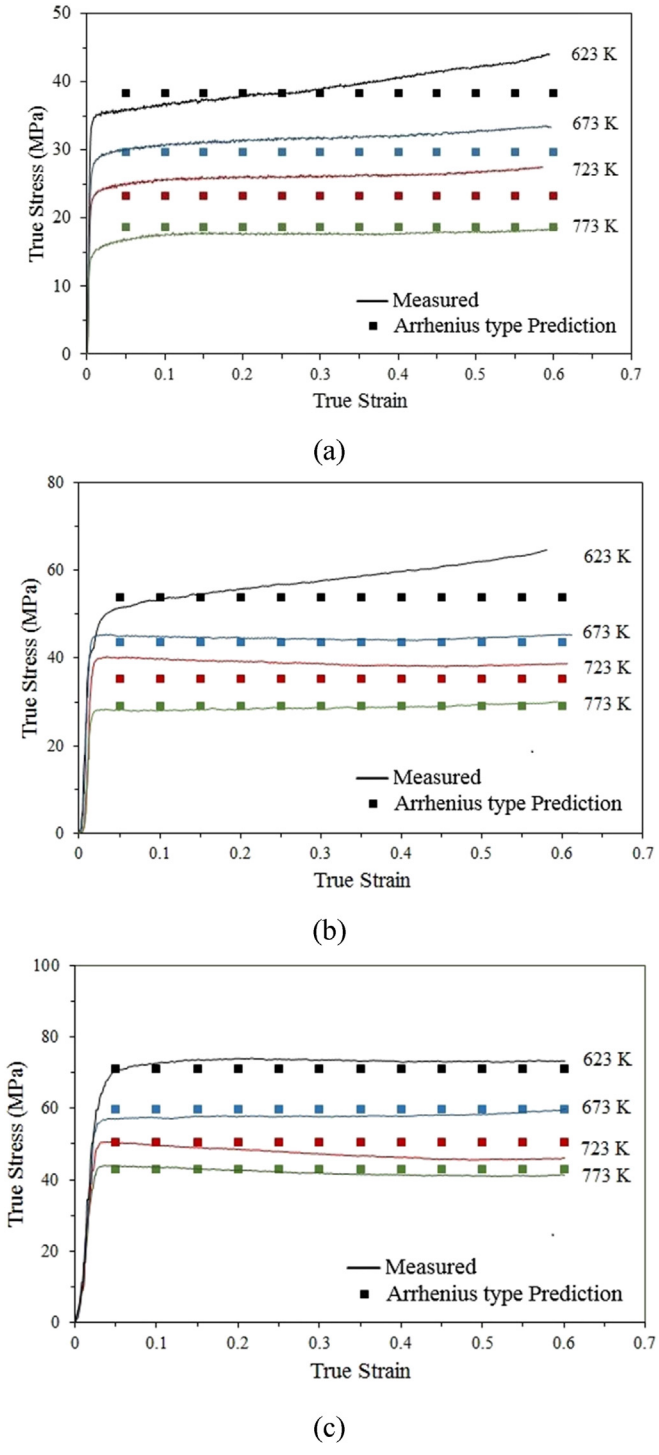

Fig. 7. Comparisons between the measured and predicted flow stress by Arrhenius-type model of AlCuMgPb alloy at strain rates of (a) 0.005 s^{-1}, (b) 0.05 s^{-1} and (c) 0.5 s^{-1}.

Fig. 7 shows the comparisons between the measured and predicted flow stress of the AlCuMgPb alloy by Arrhenius-type model at different temperature, strain and strain rate level. As it is clear from this figure, the flow stresses predicted by Arrhenius-type model agree well with the experimental results except under the strain rate of 0.005 s^{-1}, and also for the deformation temperature of 623 K.

3.2.3. Strain-compensated Arrhenius-type model

As it is clear from Fig. 2, the effect of strain is significant on the flow stress for AlCuMgPb alloy at elevated temperature of deformation, whereas this effect is not considered in the Arrhenius-type model. The results show that the strain effects on the material constants (i.e. β, α, n, A and Q) are significant in the entire strain range. Therefore, compensation strain must be considered in the Arrhenius-type model and the evaluation of material constants of this model consisting of β, α, n, lnA and Q, in order to increase the accuracy of the model prediction. The values of the material constants of the Strain-compensated Arrhenius-type model were calculated under different strains ranging from 0.05 to 0.6. So, these material constants were plotted as a function of strain, and a sixth order polynomial function was found to represent the influence of strain on material constants with a good correlation and generalization (Eq. (15)). The polynomial fit results of the materials constants and the polynomial coefficients of Eq. (15) for AlCuMgPb alloy are given in Table 2.

$$\begin{aligned}
\beta &= B_0 + B_1\varepsilon + B_2\varepsilon^2 + B_3\varepsilon^3 + B_4\varepsilon^4 + B_5\varepsilon^5 + B_6\varepsilon^6 \\
\alpha &= C_0 + C_1\varepsilon + C_2\varepsilon^2 + C_3\varepsilon^3 + C_4\varepsilon^4 + C_5\varepsilon^5 + C_6\varepsilon^6 \\
n &= D_0 + D_1\varepsilon + D_2\varepsilon^2 + D_3\varepsilon^3 + D_4\varepsilon^4 + D_5\varepsilon^5 + D_6\varepsilon^6 \\
lnA &= E_0 + E_1\varepsilon + E_2\varepsilon^2 + E_3\varepsilon^3 + E_4\varepsilon^4 + E_5\varepsilon^5 + E_6\varepsilon^6 \\
Q &= F_0 + F_1\varepsilon + F_2\varepsilon^2 + F_3\varepsilon^3 + F_4\varepsilon^4 + F_5\varepsilon^5 + F_6\varepsilon^6
\end{aligned} \tag{15}$$

The comparisons between the experimental and predicted flow stress by the Strain compensation Arrhenius-type model of the AlCuMgPb alloy at various processing conditions are shown in Fig. 8. Obviously, the Strain compensation Arrhenius-type model can appropriately describe the high-temperature flow behaviors of the AlCuMgPb alloy.

3.3. Artificial neural network model

An artificial neural network (ANN) is a mathematical or computational model that tries to simulate the structure and/or functional aspects of biological neural networks. ANN is an adaptive model that can learn from the data and generalize the things learned. Typical ANN contain an input layer, an output layer and hidden layers which are connected by the processing units called neurons and recognize patterns in a series of input and output data without any prior assumptions about their nature and interrelations, which can minimize the error between the calculated output and the experimental known targets during the training procedure. The main idea is to minimize the errors between the ANN outputs and the known targets for the corresponding inputs.

Table 2
The polynomial coefficients of β, α, n, lnA and Q for AlCuMgPb alloy.

β	α	n	lnA	Q
$B_0 = 0.1429$	$C_0 = 0.0339$	$D_0 = 3.0695$	$E_0 = 10.539$	$F_0 = 83.083$
$B_1 = 0.3924$	$C_1 = -0.0304$	$D_1 = 12.899$	$E_1 = 43.795$	$F_1 = 262.2$
$B_2 = -3.76$	$C_2 = 0.2348$	$D_2 = -115.64$	$E_2 = -290.69$	$F_2 = -1749.6$
$B_3 = 19.008$	$C_3 = -0.7499$	$D_3 = 522.94$	$E_3 = 1375.8$	$F_3 = 8359.6$
$B_4 = -48.224$	$C_4 = 1.1284$	$D_4 = -1210.5$	$E_4 = -3598.4$	$F_4 = -22{,}048$
$B_5 = 60.627$	$C_5 = -0.7246$	$D_5 = 1408.9$	$E_5 = 4933.3$	$F_5 = 30{,}403$
$B_6 = -29.994$	$C_6 = 0.0872$	$D_6 = -650.28$	$E_6 = -2687.6$	$F_6 = -16{,}623$

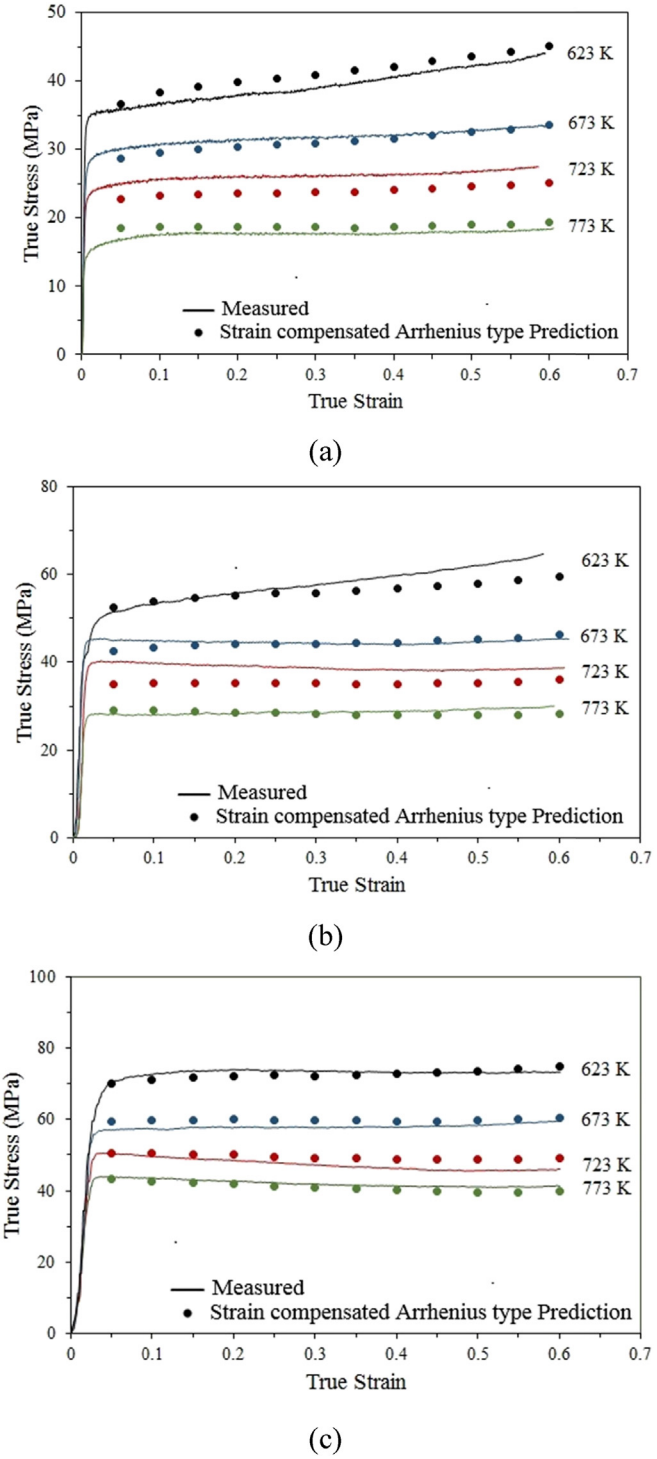

Fig. 8. Comparisons between the experimental and predicted flow stress by the Strain-compensated Arrhenius-type model of AlCuMgPb alloy at strain rates of (a) 0.005 s^{-1}, (b) 0.05 s^{-1} and (c) 0.5 s^{-1}.

In this study, a three-layer feed forward back propagation artificial neural network model has been adopted to predict the flow stress of AlCuMgPb alloy. The network consists of one input layer, three hidden layer and one output layers. The input layer has three parameters strain (ε), the logarithm of strain rate ($\ln(\dot{\varepsilon})$) and temperature (T), and the flow stress as output layer of the model. The BFGS Quasi-Newton algorithm has been employed to train this

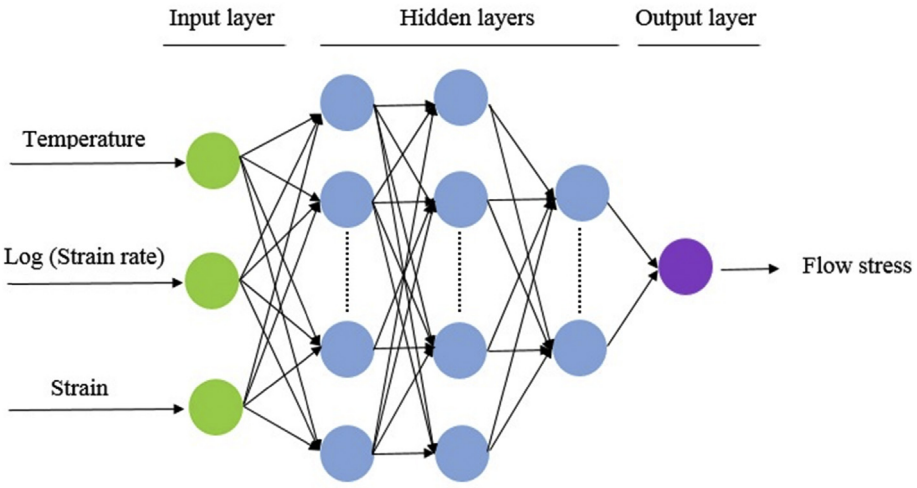

Fig. 9. The optimum structure of feed-forward ANN architecture found for present study.

network. Meanwhile, a hyperbolic tangent sigmoid transfer function has been selected to all neural units.

Fig. 9 shows the schematic diagram of the artificial neural network structure for flow stress prediction of AlCuMgPb alloy. Obviously, the determination of the appropriate number of hidden layers and number of neurons in each hidden layer is one of the most critical tasks in obtaining an accurate ANN model. The trial and error procedure is usually adopted to evaluate the optimum neural network. So several ANNs with one, two and three hidden layers have been trained and the corresponding mean square error (MSE) was calculated to check the performance of a particular architecture. After repeated trials by changing the number of neurons in the hidden layers from 1 to 15, it was discovered that a network with three hidden layers consisting of 12, 5 and 1 neurons respectively, gives the best prediction and the least error, therefore it was taken into consideration. Fig. 10 shows the training error rate of the developed ANN model. It is observed that the MSE of network decreases to the maximum epoch. As it is clear from Fig. 10, the best network performance is achieved after 500 epochs and the MSE of network is approximately constant between 500 and 800 epochs, so training epoch of 500 has been selected for this network model. Some of the ANN model features have been listed in Table 3.

In the present ANN model, the 336 data sets were selected from the true stress– true strain curves at true strain between 0.06 and 0.6 with interval of 0.02. These datasets were randomly divided into two sets: a test dataset and a training dataset. From these datasets, 68 data sets were applied to test the performance of the network model, and the other 268 datasets were used to train ANN. Before the training of the network, all input and output data should be normalized within the range from 0 to 0.9 in order to obtain a usable form for the network to read. Eq. (16) is widely used for normalization.

$$X_N = 0.1 + 0.8 \times \left(\frac{X - X_{min}}{X_{max} - X_{min}} \right) \tag{16}$$

where X is the original data, X_{min} and X_{max} are the minimum and maximum values of X respectively, X_N is the normalized data of the corresponding X.

After that the performance of the ANN model is evaluated. The flow behavior of the AlCuMgPb alloy during hot compression tests can be predicted by ANN in a wide range of temperature, strain rate and strain. Fig. 11 shows a comparison between the predicted flow stresses from ANN model and measured data from hot compression test. As it is clear, the results show that the agreement between the predicted and experimental results is very good over the full range of data and the predicted data can well track the hardening and softening regions of the hot deforming material. Therefore, the developed ANN model can be acceptably applied to simulate the hot deformation behavior of AlCuMgPb alloy.

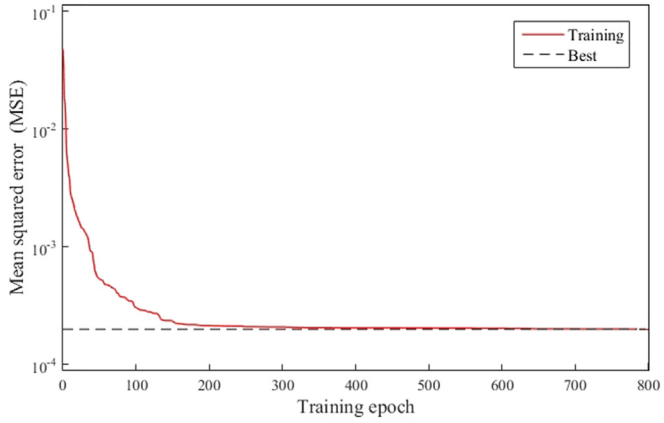

Fig. 10. Performance of the developed network at different epochs.

3.4. Comparison of the phenomenological and ANN models

The accuracy and predictability of the phenomenological and

Table 3
The features of the developed ANN model.

AAN	Parameters
Network architecture	Feed-forward back propagation
Input	Strain-temperature – log(strain rate)
Hidden neurons	12 (first hidden layer)
	5 (second hidden layer)
	1 (third hidden layer)
Output	Flow stress
Training algorithm	BFGS Quasi-Newton
Training function	Tangsig
Training performance	MSE
Training epoch	500

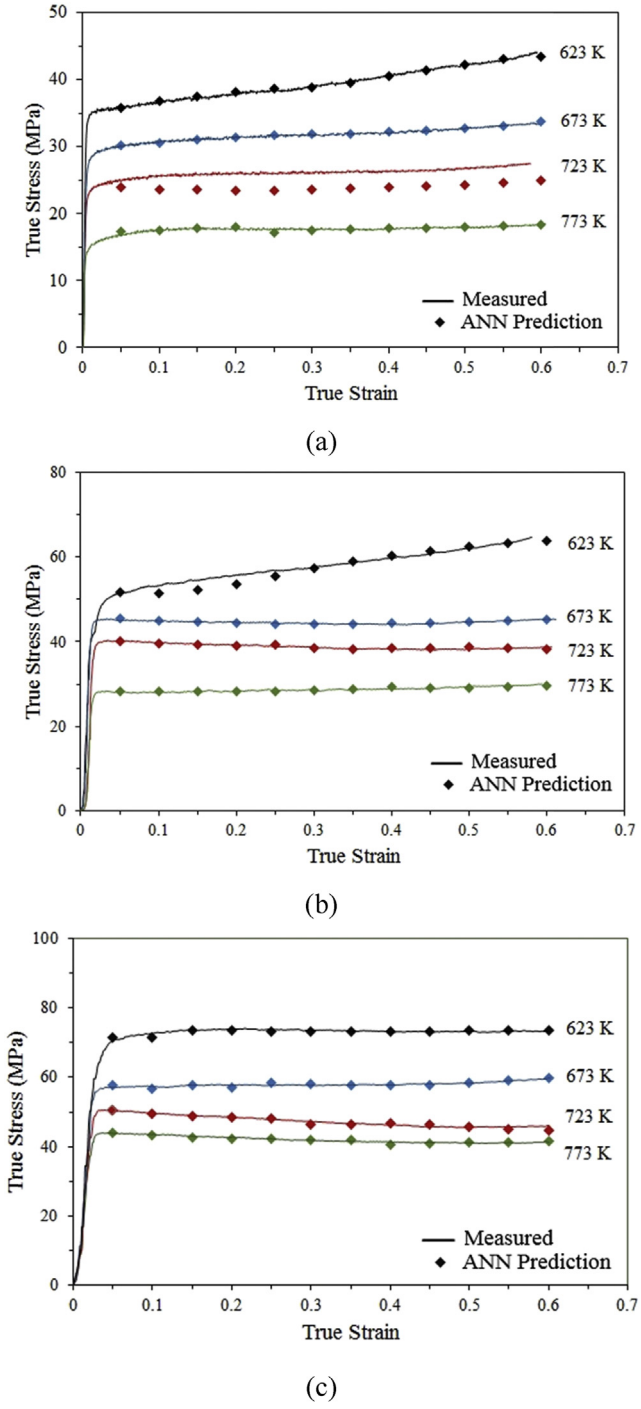

Fig. 11. Comparisons between the experimental and predicted flow stress by ANN model at strain rates of (a) 0.005 s^{-1}, (b) 0.05 s^{-1} and (c) 0.5 s^{-1}.

ANN models can be evaluated through the correlation coefficient (R) (Eq. (17)), average absolute relative error (AARE) (Eq. (18)) and root mean square error (RMSE) (Eq. (19)). They can be defined as:

$$R = \frac{\sum_{i=1}^{N}\left(\sigma_E - \overline{\sigma_E}\right)\left(\sigma_P - \overline{\sigma_P}\right)}{\sqrt{\sum_{i=1}^{N}\left(\sigma_E - \overline{\sigma_E}\right)^2 \sum_{i=1}^{N}\left(\sigma_P - \overline{\sigma_P}\right)^2}} \quad (17)$$

$$AARE(\%) = \frac{1}{N}\sum_{i=1}^{N}\left|\frac{\sigma_E - \sigma_P}{\sigma_E}\right| \times 100 \quad (18)$$

$$RMSE = \sqrt{\frac{1}{N}\sum_{i=1}^{N}(\sigma_E - \sigma_P)^2} \quad (19)$$

where σ_E is the experimental data and σ_P is the predicted value obtained from the investigated phenomenological and ANN models. $\overline{\sigma_E}$ and $\overline{\sigma_P}$ are the mean values of σ_E and σ_P respectively. N is the number of data employed in this investigation. The correlation coefficient (R) is usually used to show the linear relationship between the predicted and experimental values. However, a model may have a tendency to be biased towards lower or higher values. Therefore, the higher value of R may not always indicate better performance of the model [34]. On the other hand, the AARE and RMSE are considered as an unbiased statistics for verifying the reliability of a model. They check the predictability of a model through a term by term comparison of the relative error in prediction with respect to the actual value of the variable [35].

The correlations between the experimental flow stress data and predicted data by Johnson-Cook, Arrhenius-type, Strain-compensated Arrhenius-type and ANN models over the entire range of the strain, strain rate and temperature have been shown in Fig. 12a–d, respectively. It is clearly seen that most of the data points lie very close to the line and the correlation coefficients for the Johnson-Cook, Arrhenius-type, Strain-compensated Arrhenius-type and ANN models are 0.976, 0.985, 0.992 and 0.999, respectively. These show the Strain-compensated Arrhenius-type and ANN models have better correlation between the experimental data and predicted results compared with the Johnson-Cook and Arrhenius-type models.

Table 4 summarized the predictability of the high temperature flow stress of AlCuMgPb alloy by the investigated phenomenological and ANN models. By analysis of statistical parameters consist of R, AARE and RMSE, the calculated results show that the new developed ANN model is much better compared with the investigated phenomenological models. All of this indicates that the proposed ANN model may be efficiently utilized to predict the high temperature deformation behavior of AlCuMgPb aluminum alloy with reasonable accuracy and reliability.

Fig. 13 shows the values of average absolute relative error (AARE) at different strains for the developed models. It can be seen that the AAREs obtained from the Johnson-Cook model are greatly higher than the ones obtained from the other models at all strain ranges considered in this investigation. The results show that the Strain-compensated Arrhenius-type model has better correlation between the predicted results and experimental data compared with the other studied phenomenological models. Also, it is clear that the AAREs of the ANN model have the least value in comparison to the investigated phenomenological models.

Furthermore, the performance of the developed models is investigated by statistical analysis of the relative error. The predictions are compared with the corresponding experimental data and subsequently the relative errors are calculated as Eq. (20).

$$\text{Relative Error}(\%) = \left(\frac{\sigma_E - \sigma_P}{\sigma_E}\right) \times 100 \quad (20)$$

where σ_E and σ_P have the same meaning as stated earlier. The comparison of relative error between the experimental and predicted flow stress by ANN model and phenomenological models at strain of 0.5 have been shown graphically as scatter in Fig. 14. It can

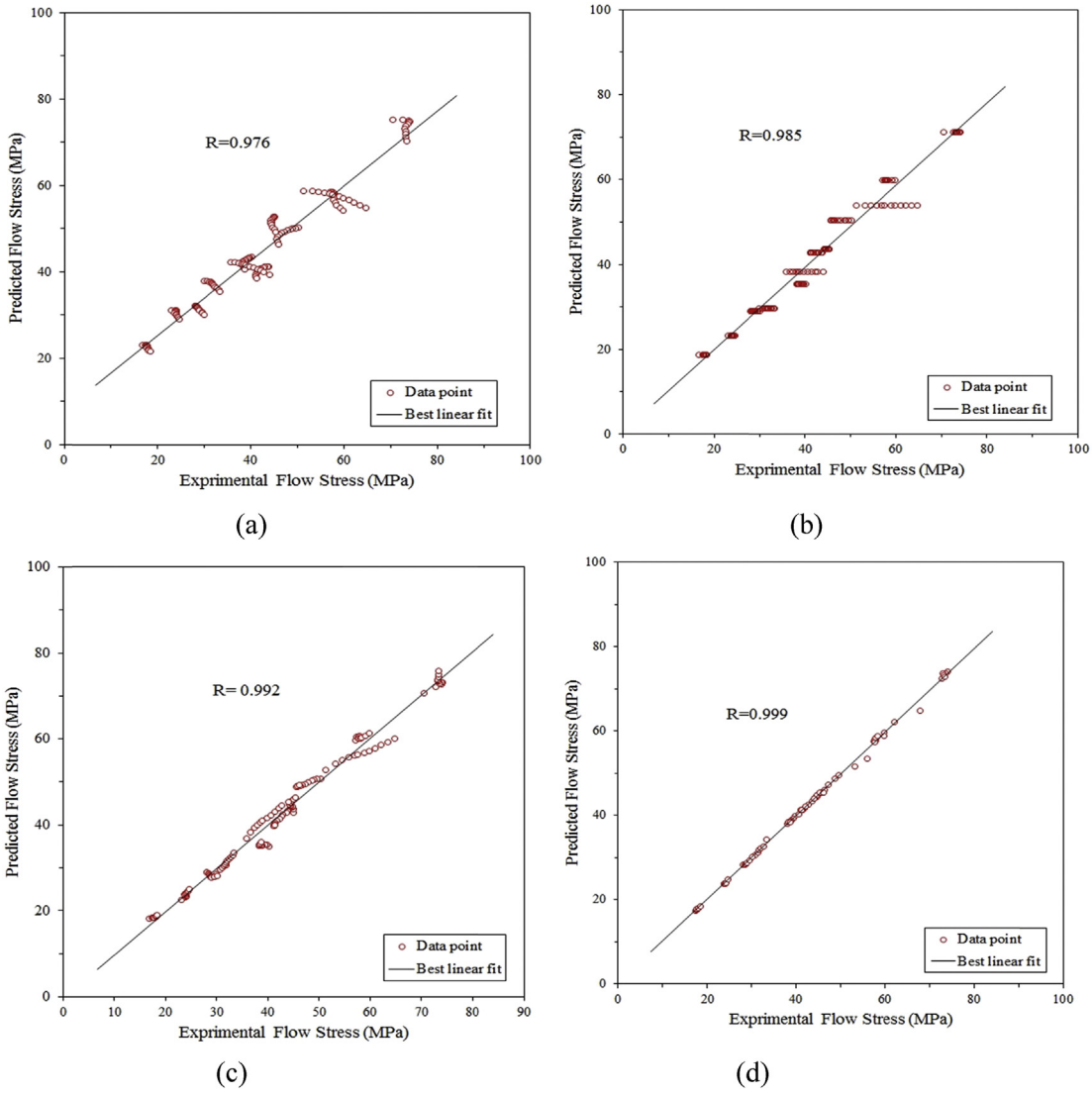

Fig. 12. Correlation between the experimental and predicted flow stress values by the (a) Johnson-Cook, (b) Arrhenius-type, (c) Strain-compensated Arrhenius-type and (d) ANN models.

be seen that the relative error obtained from the ANN model varies from −1.075% to 1.075% whereas it is in ranges of −6.795% to 7.685%, −10.58%–15.01% and −18.06% to 15.289% for the Strain-compensated Arrhenius-type, Arrhenius-type and Johnson-Cook models, respectively. In the other word, the ANN, Strain-compensated Arrhenius-type, Arrhenius-type and Johnson-Cook models give the best performance for the prediction of hot deformation behavior of AlCuMgPb alloy, sequentially.

All the above results clearly indicate that the obtained artificial neural networks model showed very good performance and could be applied to predict the hot flow behavior of AlCuMgPb aluminum alloy more accurately than the investigated phenomenological models. This is because the deformation behavior of the materials is very nonlinear under elevated temperatures and strain-rates,

Table 4
The calculated values of R, AARE and RMSE for the developed models.

Model	R	AARE (%)	RMSE (MPa)
Johnson-Cook	0.976	10.978	4.285
Arrhenius-type	0.985	4.819	7.226
Strain-compensated Arrhenius-type	0.992	3.577	3.386
ANN	0.999	0.65	0.315

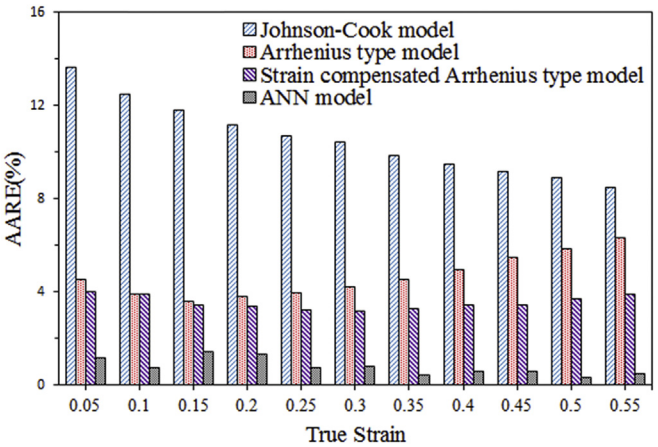

Fig. 13. The average absolute relative error (AARE) for the developed phenomenological and ANN models at various true strains.

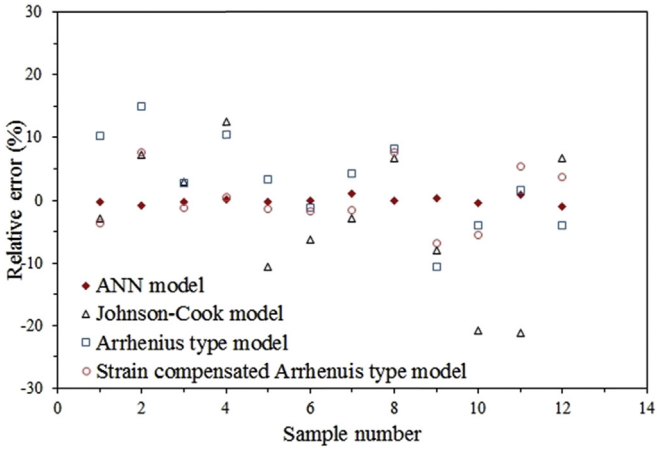

Fig. 14. Comparison of relative error (%) between the experimental and predicted flow stress by ANN model and investigated phenomenological models at strain of 0.5.

which this condition decreases the prediction accuracy of the flow stress by the constitutive equations and limits the applicable range.

4. Conclusions

A comparative investigation has been made on the capability of the ANN model and the phenomenological constitutive models consist of Strain-compensated Arrhenius-type, Arrhenius-type and Johnson-Cook models to describe the elevated temperature flow behavior of AlCuMgPb alloy in the temperature range of 623–773 K and with the strain rate of 0.005–0.5 s^{-1}. Based on this study, the following conclusions can be drawn:

- The flow stress increases with increasing strain rate and decreases with increasing the deformation temperature, and strain has significant influence on the flow stress.
- The artificial neural network (ANN) model and the phenomenological constitutive models consist of Johnson-Cook, Arrhenius-type and Strain-compensated Arrhenius-type models were obtained. A fairly good agreement has been obtained between the flow stress values predicted by the Johnson-Cook constitutive equation and the experimental results. The Arrhenius-type constitutive equation could predict the flow stress accurately except under the strain rate of 0.005 s^{-1}. The Strain-compensated Arrhenius-type constitutive equation could represent the elevated temperature flow behavior more accurately than the other investigated phenomenological models consist of Johnson-Cook and Arrhenius-type constitutive equations in the entire processing domain. Among the ANN and the investigated phenomenological models, the developed artificial neural network model shows the most excellent capability to track the hot deformation behavior throughout the entire temperature, strain and strain rate range.
- It is obtained that the correlation coefficients from the Johnson-Cook, Arrhenius-type, Strain-compensated Arrhenius-type and artificial neural network models are 0.976, 0.985, 0.992 and 0.999 respectively, and the average absolute relative errors are 10.98%, 4.82%, 3.58% and 0.65% correspondingly. The relative errors obtained from the Johnson-Cook, Arrhenius-type and Strain-compensated Arrhenius-type models vary from −18.06% to 15.289%, −10.58%–15.01% and −6.795% to 7.685% respectively, whereas it is in the range of −1.075% to 1.075% for the artificial neural network model.
- In terms of the average absolute relative error of prediction, root mean square error, correlation coefficient, and the capability to track the high-temperature flow behavior, the ANN model could provide an effective choice to predict the hot deformation behavior. Moreover it is not necessary to assume a mathematical model at first or identify its parameters using an artificial neural network, which make it more effective than the constitutive equations. However, it is strongly dependent on comprehensive high quality experimental data and characteristic variables, and this model gives no physical insight.

References

[1] Y.C. Lin, Q.F. Li, Y.C. Xia, L.T. Li, A phenomenological constitutive model for high temperature flow stress prediction of Al–Cu–Mg alloy, Mater. Sci. Eng. A 534 (2012) 654–662.
[2] J. Malas, S. Venugopal, T. Seshacharyulu, Effect of microstructural complexity on the hot deformation behavior of aluminum alloy 2024, Mater. Sci. Eng. A 368 (2004) 41–47.
[3] X. Huang, H. Zhang, Y. Han, W. Wu, J. Chen, Hot deformation behavior of 2026 aluminum alloy during compression at elevated temperature, Mater. Sci. Eng. A 527 (2010) 485–490.
[4] H.R. Rezaei Ashtiani, M.H. Parsa, H. Bisadi, Constitutive equations for elevated temperature flow behavior of commercial purity aluminum, Mater. Sci. Eng. A 545 (2012) 61–67.
[5] Y. Lin, M.S. Chen, J. Zhong, Prediction of 42CrMo steel flow stress at high temperature and strain rate, Mech. Res. Com. 35 (2008) 142–150.
[6] B. Wu, M. Li, D. Ma, The flow behavior and constitutive equations in isothermal compression of 7050 aluminum alloy, Mater. Sci. Eng. A 542 (2012) 79–87.
[7] Y. Lin, Y.C. Xia, X.M. Chen, M.S. Chen, Constitutive descriptions for hot compressed 2124-T851 aluminum alloy over a wide range of temperature and strain rate, Comput. Mater. Sci. 50 (2010) 227–233.
[8] C. Shi, W. Mao, X.G. Chen, Evolution of activation energy during hot deformation of AA7150 aluminum alloy, Mater. Sci. Eng. A 571 (2013) 86–91.
[9] J.H. Guo, S.D. Zhao, G.H. Yan, Z.B. Wang, Novel flow stress model of AA 4343 aluminium alloy under high temperature deformation, Mater. Sci. Tech. 29 (2013) 197–203.
[10] W. Li, H. Li, Z. Wang, Z. Zheng, Constitutive equations for high temperature flow stress prediction of Al–14Cu–7Ce alloy, Mater. Sci. Eng. A 528 (2011) 4098–4103.
[11] G. Chen, G. Fu, S. Lin, C. Cheng, W. Yan, H. Chen, Simulation of flow of aluminium alloy 3003 under hot compressive deformation, Metal. Sci. Heat. Treat. 54 (2013) 623–627.
[12] L. Ou, Y. Nie, Z. Zheng, Strain compensation of the constitutive equation for high temperature flow stress of a Al-Cu-Li alloy, J. Mater. Eng. Perf. 23 (2014) 25–30.
[13] H.Y. Li, Y.H. Li, X.F. Wang, J.J. Liu, Y. Wu, A comparative study on modified Johnson Cook, modified Zerilli–Armstrong and Arrhenius-type constitutive models to predict the hot deformation behavior in 28CrMnMoV steel, Mater. Des. 49 (2013) 493–501.
[14] Y. Lin, X.M. Chen, A critical review of experimental results and constitutive descriptions for metals and alloys in hot working, Mater. Des. 32 (2011) 1733–1759.
[15] H. Shin, J.B. Kim, A phenomenological constitutive equation to describe various flow stress behaviors of materials in wide strain rate and temperature regimes, Eng. Mater. Tech. 132 (2010) 1–6.
[16] A. Rusinek, J. Rodríguez-Martínez, A. Arias, A thermo-viscoplastic constitutive model for FCC metals with application to OFHC copper, Inter. J. Mech. Sci. 52 (2010) 120–135.
[17] G.R. Johnson, W.H. Cook, A constitutive model and data for metals subjected to large strains, high strain rates and high temperatures, Eng. Fract. Mech. 21 (1985) 1–31.
[18] J.J. Jonas, C.M. Sellars, W. J. MeG. Tegart, Strength and structure under hot-working conditions, Metall. Rev. 14 (1969) 1–24.
[19] M. Mostafaei, M. Kazeminezhad, Hot deformation behavior of hot extruded Al–6Mg alloy, Mater. Sci. Eng. A 535 (2012) 216–221.
[20] J. Zhang, B. Chen, B. Zhang, Effect of initial microstructure on the hot compression deformation behavior of a 2219 aluminum alloy, Mater. Des. 34 (2012) 15–21.
[21] F. Slooff, J. Zhou, J. Duszczyk, L. Katgerman, Constitutive analysis of wrought magnesium alloy Mg–Al4–Zn1, Scr. Mater. 57 (2007) 759–762.
[22] J. Li, F. Li, J. Cai, R. Wang, Z. Yuan, F. Xue, Flow behavior modeling of the 7050 aluminum alloy at elevated temperatures considering the compensation of strain, Mater. Des. 42 (2012) 369–377.
[23] G.F. Xu, X.-Y. Peng, X.P. Liang, X. Li, Z.M. Yin, Constitutive relationship for high temperature deformation of Al-3Cu-0.5Sc alloy, Trans. Nonferr. Metals Soc. China 23 (2013) 1549–1555.
[24] Y. Lin, M.S. Chen, J. Zhong, Constitutive modeling for elevated temperature flow behavior of 42CrMo steel, Comput. Mater. Sci. 42 (2008) 470–477.
[25] S. Mandal, V. Rakesh, P. Sivaprasad, S. Venugopal, K. Kasiviswanathan,

Constitutive equations to predict high temperature flow stress in a Ti-modified austenitic stainless steel, Mater. Sci. Eng. 500 (2009) 114–121.
[26] R.X. Chai, C. Guo, L. Yu, Two flowing stress models for hot deformation of XC45 steel at high temperature, Mater. Sci. Eng. 534 (2012) 101–110.
[27] Y.J. Qin, Q.L. Pan, Y.B. He, W.B. Li, X.Y. Liu, X. Fan, Artificial neural network modeling to evaluate and predict the deformation behavior of ZK60 magnesium alloy during hot compression, Mater. Manu. Proc. 25 (2010) 539–545.
[28] O. Sabokpa, A. Zarei-Hanzaki, H. Abedi, N. Haghdadi, Artificial neural network modeling to predict the high temperature flow behavior of an AZ81 magnesium alloy, Mater. Des. 39 (2012) 390–396.
[29] N. Haghdadi, A. Zarei-Hanzaki, A. Khalesian, H. Abedi, Artificial neural network modeling to predict the hot deformation behavior of an A356 aluminum alloy, Mater. Des. 49 (2013) 386–391.
[30] Z. Lu, Q. Pan, X. Liu, Y. Qin, Y. He, S. Cao, Artificial neural network prediction to the hot compressive deformation behavior of Al–Cu–Mg–Ag heat-resistant aluminum alloy, Mech. Res. Com. 38 (2011) 192–197.
[31] H.Y. Li, X.F. Wang, D.D. Wei, J.D. Hu, Y.H. Li, A comparative study on modified Zerilli–Armstrong, Arrhenius-type and artificial neural network models to predict high-temperature deformation behavior in T24 steel, Mater. Sci. Eng. A 536 (2012) 216–222.
[32] X. Xiao, G. Liu, B. Hu, X. Zheng, L. Wang, S. Chen, A. Ullah, A comparative study on Arrhenius-type constitutive equations and artificial neural network model to predict high-temperature deformation behaviour in 12Cr3WV steel, Comput. Mater. Sci. 62 (2012) 227–234.
[33] ASTM E209, Standard practice for compression tests of metallic materials at elevated temperatures with conventional or rapid heating rates and strain-rates, in: Annual Book of ASTM Standards, vol. 03.01, 2010.
[34] P.M. Phaniraj, K.A. Lahiri, The applicability of neural network model to predict flow stress for carbon steels, J. Mater. Proc. Tech. 141 (2003) 219–227.
[35] S. Srinivasulu, A. Jain, A comparative analysis of training methods for artificial neural network rainfall–runoff models, Appl. Soft Comput. 6 (2006) 295–306.